***JKPK (JURNAL KIMIA DAN PENDIDIKAN KIMIA)**, Vol. 8, No.1, 2023* *pp. 86-100*
Chemistry Education Study Program, Universitas Sebelas Maret *ISSN 2503-4146*
https://jurnal.uns.ac.id/jkpk *ISSN 2503-4154 (online)*

EVALUATION OF COLOR MODELS FOR QUANTITATIVE DETERMINATION OF FOOD DYES USING SMARTPHONE-BASED DIGITAL IMAGE ANALYSIS

Giovania Evangeline Halim and Martin Tjahjono*

Department of Chemical and Food Processing, Calvin Institute of Technology, Jakarta, Indonesia
Calvin Tower RMCI Jl. Industri Blok B14, Jakarta

* Correspondence, email: martin.tjahjono@calvin.ac.id

Received: March 8, 2023 Accepted: April 29, 2023 Online Published: April 30, 2023
DOI : 10.20961/jkpk.v8i1.72928

ABSTRACT

In recent years, smartphones for digital image analysis (DIA) have emerged as an affordable, user-friendly, and accessible chemical and food analysis tool, particularly in colorimetry. This study aimed to compare the performance of various color models and demonstrate their usefulness in quantifying food dyes in commercial products using DIA. Images of food dye solutions at 500 Lux were captured using an OPPO F11 smartphone, and the RGB values are mathematically transformed into several color models. The results show that the normalized blue channel was the most robust color model for analyzing different food dyes using DIA. The corresponding limit of detection (LOD) and limit of quantification (LOQ) for nine food dyes studied are following: carmoisine, 3.7 and 11.3 mg/L; sunset yellow, 1.0 and 3.1 mg/L; allura red, 2.0 and 6.0 mg/L; ponceau 4R, 1.3 and 4.0 mg/L; tartrazine, 5.0 and 15.2 mg/L; fast green, 2.0 and 6.1 mg/L; brilliant blue, 1.9 and 5.7 mg/L; quinoline yellow WS, 3.3 and 9.9 mg/L and indigo carmine, 1.2 and 3.8 mg/L. These LOD and LOQ values were comparable to those obtained from UV-Vis spectroscopy measurements: carmoisine, 2.4 and 7.2 mg/L; sunset yellow: 0.9 and 2.6 mg/L; allura red, 1.4 and 4.2 mg/L; ponceau 4R, 1.9 and 5.7 mg/L; tartrazine, 0.9 and 2.7 mg/L; fast green, 1.5 and 4.4 mg/L; brilliant blue, 3.6 and 10.9 mg/L; quinoline yellow WS, 0.3 and 0.9 mg/L and indigo carmine, 4.3 and 13.0 mg/L. The DIA method was successfully applied to determine the concentrations of food dyes in three commercial samples (Samples S1-S3) containing carmoisine, tartrazine, and brilliant blue, respectively. The measured concentrations are 52.7±2.6 mg/L (S1), 105.9±5.4 mg/L (S2) and 7.9±0.5 mg/L (S3), which are in good agreement with UV-Vis spectroscopy results employing standard addition method 58.2±3.0 mg/L (S1), 106.2±1.3 mg/L (S2), 8.3±0.5mg/L (S3). Overall, this color model study demonstrates the utility of DIA method as a reliable and affordable food dye analysis tool that can potentially be used for public health and safety monitoring.

Keywords: *Digital image-based analysis, smartphone, food dye, color model, UV-Vis Spectroscopy.*

INTRODUCTION

Over the last decade, built-in smartphone cameras have replaced regular point-and-shoot digital cameras. The imaging capabilities of smartphone cameras have improved continuously, allowing them to capture high-resolution images suitable for physical, chemical, and biological assessment based on their color information using colorimetry [1] or fluorescence analysis [2].

In food analysis, digital image-based analysis (DIA) using smartphones has been utilized to quantify various food chemicals, such as phenols [3], nitrites [4], and alcohols [5]. Several other studies have demonstrated that smartphones can detect microbial contaminants and adulteration in dairy products [6] and assess the quality and freshness of fruits and vegetables [7,8]. In addition, DIA offers some practical advantages such as simplicity, accessibility, and affordability [9].

However, DIA requires special attention to achieve accurate and precise measurements. This includes capturing good quality and consistent images of the objects without interference or minimal changes in ambient light, obtaining raw digital data from a smartphone to avoid demosaicing images, and extracting meaningful information using correlations to the corresponding color model parameters. In addition, selecting appropriate color model parameters is important for obtaining reliable information from colored objects.

Most digital images display color information in the RGB because camera sensors detect color through red, green, and blue filters. However, the RGB color space is sensitive to changes in illumination and tends to produce unstable color signals under varying lighting conditions [10,11]. This sensitivity can affect the accuracy and precision of discriminating analyte color changes. Therefore, analysis using color model parameters independent of changes in lighting conditions is preferable for DIA measurements. Various color model parameters have been previously used in recent DIA studies, including the decadic logarithm function of the RGB signals based on Beer-Lambert Law [12,13], normalized RGB [14], combined RGB [13,15] and the conversion of RGB values into HSL (hue, saturation, lightness) color space [16]. However, while the DIA studies mentioned above have demonstrated the utility of their models for quantitative analysis, these models were generally applied to limited color samples. Furthermore, few previous works have provided a clear explanation on why a particular color model was chosen to analyze the sample or why a specific color channel could outperform the others in the analysis.

This research aims to fill the above gap by examining the performance of various color models using DIA. Additionally, this study demonstrates the usefulness of DIA using smartphones to quantify food dyes in commercial products. In this regard, six different color models are evaluated to determine the most reliable color model that achieves the lowest limit of detection (LOD) and limit of quantification (LOQ) from DIA measurements. The models are compared on various food dyes with different color settings. Nine synthetic food dyes commonly used in food and beverage products carmoisine, sunset yellow, allura red, ponceau 4R, tartrazine, fast green, brilliant blue, quinoline yellow WS and indigo carmine, are studied to demonstrate the DIA methodology. These food dyes represent different colors and chemical group structures, namely monoazo, triarylmethane, quinoline, and indigoid dyes. The limit of detection (LOD) and quantification (LOQ) resulting from DIA measurements using the best model is determined and compared to those obtained from a more established UV-Vis spectroscopy technique. Subsequently, the

best-performing color model is applied to measure food dye concentrations in commercial products.

METHOD

Materials

This study investigated nine commercial-grade synthetic food dyes manufactured by Neelikon (Mumbai, India), the most used synthetic colorants in commercial food and health products. The dyes investigated in this study include carmoisine, sunset yellow, allura red, ponceau 4R, tartrazine, fast green, brilliant blue, quinoline yellow WS and indigo carmine, and are summarized in Table 1.

Table 1. List of synthetic food dyes used in this study.

Color Index (CI) Number	Name	Structure	Purity (%)[1]	λ (nm)[2]	λ_{ref} (nm)
14720	Carmoisine	Monoazo	94.50	516	516 [17]
15985	Sunset Yellow	Monoazo	89.55	482	482 [18]
16035	Allura Red	Monoazo	90.26	504	505 [19]
16255	Ponceau 4R	Monoazo	88.37	508	508 [20]
19140	Tartrazine	Monoazo	90.87	426	426 [21]
42053	Fast Green	Triarylmethane	92.21	626	624 [22]
42090	Brilliant Blue	Triarylmethane	89.95	630	630 [23]
47005	Quinoline Yellow WS	Quinoline	72.08	412	415 [24]
73015	Indigo Carmine	Indigoid	90.37	612	612 [25]

[1] As specified by the products' certificate of analysis from the manufacturer.
[2] UV-Vis absorption maxima, measured in this study.

Three different commercial products were used as model solutions: strawberry-flavoured soda (S1), energy drink (S2), and blueberry-flavoured soda (S3). Each model solution contains only one type of dye: carmoisine (S1), tartrazine (S2) and brilliant blue (S3). These samples were purchased from local convenience stores in Jakarta, Indonesia.

Preparation of Standard Solutions and Samples

To prepare the stock solutions for each dye, 100.0±0.2 mg of dye powder was weighed using an analytical balance (Sartorius Entris 224i-1S) dissolved in a 100.0±0.1 mL volumetric flask (Iwaki, Japan) using ultrapure water (Adrona B30 HPLC system, Riga, Latvia) to obtain a concentration of approximately 1000 mg/L. Standard solutions for external calibration were prepared by pipetting the appropriate amount of stock solution using a 1000±6 µL micropipette (Corning, New York) into a separate volumetric flask (100.0±0.1 mL, Grade A, Iwaki, Japan) and then diluting them with ultrapure water.

The three commercial samples used in this study were clear beverage solutions. Samples S1 and S3 contained soda and were degassed before analysis to avoid interference with the color measurements. Sample S2 did not require any prior treatment and could be directly analyzed. However, the dye concentrations in Samples S1 and S2 exceeded the range of their corresponding calibration curves, requiring 5-10 times dilution to obtain more accurate results for the analysis.

The analytical solutions were placed in 12 x 12 x 45 mm polystyrene cuvettes (Kartell, Italy) with a 10 mm path length for DIA and UV-Vis spectroscopy measurements. Each sample was measured in triplicates.

Data Collection

For digital image analysis (DIA), unprocessed images in digital negative (DNG) file formats were acquired using OPPO F11 smartphone and Adobe Lightroom v7.4.1 (Adobe), without flash. This procedure was necessary to obtain raw digital data from the smartphone and avoid demosaicing the images.

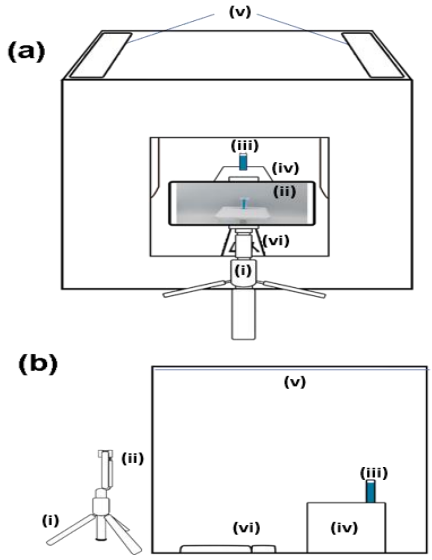

Figure 1. (a) Front and (b) side view of the photobox setup, consisting of a (i) tripod (ii) smartphone, (iii) cuvette, (iv) elevation stand, (v) two 30w 5500K LED light strips as light source, and (vi) a lux meter.

Sample solutions were placed inside a 40 cm x 40 cm Puluz PU5060 photo box, equipped with two 30w 5500K LED light strips with adjustable intensity. This provided a consistent illumination condition with minimum interference from ambient light. Images were taken at constant 500±5 Lux measured using AS803 Lux Meter, approximating typical office room lighting. Figure 1 shows the experimental setup for DIA measurement in this study.

The smartphone was positioned on a fixed 16.5 cm tripod at 0° inclination to ensure consistent image capture directly in front of the photo box. A polystyrene cuvette containing the dye solution was positioned approximately 25 cm from the light source, 6 cm from the white background, and 36.5 cm from the smartphone camera. To ensure consistent reflection of the color, the cuvette was placed on top of a 12 cm white box, aligning its height with the smartphone camera lens. The resulting raw images were transferred to a computer. RGB values were extracted from a region of interest (ROI) of approximately 1000 pixels using Adobe Photoshop CS6.

UV-Vis spectroscopy measurements were conducted using a single-beam spectrophotometer (Hanon Instruments, i3) with a deuterium light source to validate the DIA results. The spectrophotometer was used to scan the food dye solutions from 380 nm to 700 nm and determine each food dye solution's maximum absorbance wavelength (λ_{max}) (refer to Table 1). The λ_{max} values were then used to quantify the absorbance values of the food dye solutions.

Additionally, a single-point standard addition method [26] was used to analyze the commercial samples with the UV-Vis spectrophotometer, demonstrating that there was no significant interaction between the food dye and other ingredients in the model solutions that could have hindered the quantitative analysis of the dye.

Constructing Standard Calibration Curves Using Various Color Models

A total of six quantitative color models were compared in this work to evaluate the most reliable linear model, which provides the lowest limit of detection (LOD) and limit of quantification (LOQ) in quantifying food dye

concentrations in solutions. A standard calibration curve was constructed for each color model by plotting the associated color parameter against the standard concentration of the dye. The coefficient of determination (r^2), limit of detection (LOD) and limit of quantification (LOQ) were subsequently calculated from the corresponding linear regression. A robust color model would have a high r^2 value (close to 1.0) and low LOD and LOQ values. The details of each color model compared in this work are explained below.

Model 1 is a logarithmic color model based on the Lambert-Beer Law, as expressed in Eq. (1):

$$A = -Log\frac{I}{I_0} \quad \text{……(1)}$$

I_0 is the signal intensity of the R, G or B channel obtained from the blank solution, and I is the corresponding R, G or B signal intensity of the standard or sample solution. Subsequently, the red-channel, green-channel and blue-channel color parameters can be evaluated using Eq. (1), and they are represented as Model 1a, Model 1b and Model 1c, respectively. Model 1 is one of the most ubiquitous models used for quantitative analysis in digital image-based colorimetry. This logarithmic color model has been used in previous studies to quantify iron and chromium ion concentration in solutions [12] and to analyze ascorbic acid concentration in fruit juices [27].

Model 2 utilizes the analytical signal (S_i), where the digital signal (I) of each R, G or B color channel of the image is subtracted from the maximum intensity (i.e. 255) of the color space:

$$S_i = 255 - I \quad \text{……(2)}$$

Subsequently, the red-channel, green-channel and blue-channel color parameters can be evaluated using Eq. (2) and represented as Model 2a, Model 2b and Model 2c, respectively..

Model 3 is a modified logarithmic color parameter derived from Model 1 (Eq. (1)). However, unlike Model 1, which used the individual R, G or B channel to represent the I and I_0 values, Model 3 calculated the average RGB values of the blank (I_0) and standard or sample solution (I), using Eq. (3):

$$I = \frac{1}{3}(R + G + B) \quad \text{……(3)}$$

Model 4 is known as the surface color index (I_{sc}) model. This model was used to quantify total protein concentration of bovine serum albumin [15]. The surface color index can be calculated using Eq. (4), dividing a magnification factor (k =10^5) by the sum of the RGB vectors.

$$I_{sc} = \frac{k}{(R^2+G^2+B^2)^{\frac{1}{2}}} \quad \text{……..….(4)}$$

Model 5 is a normalized form of the RGB color model. The normalized RGB parameters (r, g or b) are calculated from Eqs. (5a-c) for red-channel, green-channel and blue-channel, respectively. The normalized form of the RGB color model was introduced as a simple and versatile tool for at-home laboratory learning module [14].

$$r = \frac{R}{R+G+B} \quad \text{……...(5a)}$$

$$g = \frac{G}{R+G+B} \quad \text{……..(5b)}$$

$$b = \frac{B}{R+G+B} \quad \text{……...(5c)}$$

In contrast to Models 1-5, performed in RGB color space, Model 6 uses the HSL (Hue, Saturation, Lightness) color space, which has been described as being light insensitive compared to the RGB space [28].

The measured digital values of red, green or blue channels in RGB color space were transformed into H, S and L color parameters using Eqs. (6-8). Saturation (*S*) and lightness (*L*) color parameters are represented as Model 6a and 6b, respectively. Hue (*H*) is not suitable for quantitative analysis as this parameter is considered to be insensitive to concentration changes [29].

$$\frac{1}{60}H = H' = \begin{cases} \left(\frac{G'-B'}{\Delta} + 0\right) mod6 \;\; if\; M = R' \\ \left(\frac{B'-R'}{\Delta} + 0\right) mod6 \; if\; M = G' \\ \left(\frac{R'-G'}{\Delta} + 0\right) mod6 \; if\; M = B' \end{cases}$$

$$R' = \frac{R}{255}$$

$$G' = \frac{G}{255}$$

$$B' = \frac{B}{255} \qquad \text{.....(6)}$$

$$M = max(R', G', B')$$

$$m = min(R', G', B')$$

$$\Delta = M - m$$

$$L = \frac{M-m}{2} \qquad \text{.....(7)}$$

$$S = \begin{cases} 0 & if\; L \in \{0,1\} \\ \frac{\Delta}{1-|2L-1|} & if\; L \notin \{0,1\} \end{cases} \text{.....(8)}$$

RESULTS AND DISCUSSION

Assessment of Color Models

To evaluate the performance of the six color models (Models 1 to 6), standard solutions of carmoisine (red, monoazo), brilliant blue (blue, trialrymethane), tartrazine (yellow, monoazo), quinoline yellow WS (yellow, quinoline), and indigo carmine (blue, indigoid) were analyzed individually. These five food dyes were chosen to represent the different primary dye colors (red, blue, yellow) and four chemical structures of common food dyes. Two pairs of similarly colored dyes with different chemical structures, namely tartrazine and quinoline yellow WS, and brilliant blue and indigo carmine, were selected to investigate whether the performance of the different models was influenced by the substances' color or chemical structures.

The concentration was plotted against parameter from the six color models for each selected food dye. The coefficient of determination (r^2) obtained from linear regression analysis was used to evaluate the goodness of fit of each color model. Figure 2 shows an inverse correlation between r^2 value and its LOD. This implies that a model with higher r^2 value can detect the desired analytes with greater sensitivity and hence quantify the substance more accurately as represented by LOQ, which is approximately 3.3 times of LOD.

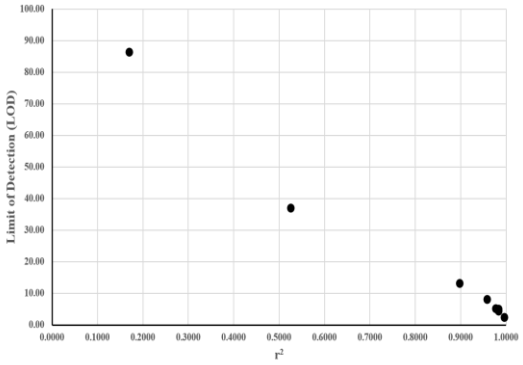

Figure 2. Inverse relationship between r^2 values obtained from linear regression analysis and its limit of detection (LOD). The higher r^2 value results in lower LOD and hence provides a higher accuracy of measurement.

The results in Table 2 show that the performance of Models 1 and 2 is highly influenced by the color of the dyes. Typically, the best performing color channel is the one that is opposite or complementary to the perceived color of the solution. For instance, Models 1c and 2c, which represent the blue channel, performed well on red (carmoisine)

and yellow (quinoline yellow and tartrazine) dyes but showed poor performance when used on blue dyes (brilliant blue and indigo carmine).

Table 2. The coefficient of determination (r^2) of various color models, performed on five food dye solutions within concentration range given in brackets.

Color Model	Carmoisine (0-50 mg/L)	Brilliant Blue (0-20 mg/L)	Tartrazine (0-30 mg/L)	Quinoline Yellow WS (0-25 mg/L)	Indigo Carmine (0-50 mg/L)	Average r^2
1a	0.9110	0.9761	0.5257	0.1462	0.9571	0.7032
1b	0.9678	0.9880	0.1694	0.2000	0.9512	0.6553
1c	0.9959	0.3344	0.9959	0.9728	0.1351	0.6868
2a	0.9105	0.9669	0.5193	0.1460	0.9856	0.7057
2b	0.8902	0.9864	0.1672	0.1989	0.9429	0.6371
2c	0.9547	0.3308	0.9671	0.9763	0.1394	0.6737
3	0.9758	0.9925	0.9580	0.7432	0.9600	0.9259
4	0.9787	0.9615	0.8978	0.7102	0.9524	0.9001
5a	0.9801	0.9945	0.9842	0.9921	0.9921	0.9886
5b	0.9270	0.9895	0.9815	0.9914	0.9513	0.9681
5c	**0.9971**	**0.9959**	**0.9831**	**0.9918**	**0.9997**	**0.9935**
6a	0.9479	0.9990	0.9836	0.9855	0.9917	0.9815
6b	0.9291	0.9756	0.9773	0.8712	0.9583	0.9423

Models 1 and 2 rely on the individual R, G, or B channel for analysis, while Models 3 and 4 utilize combined RGB parameters (see Eqs. (3) and (4)). Compared to Models 1 and 2, Models 3 and 4 perform significantly better, with average r^2 values of 0.9259 and 0.9001, respectively. However, it is worth noting that Models 3 and 4 produce relatively lower r^2 values in yellow dyes, indicating that they are still somewhat dependent on dye color.

Models 5a-c are normalized RGB models that use all channel information for analysis and outperform other RGB-based models (Models 1-4). The average r^2 values in five different food dyes are 0.9886, 0.9681 and 0.9935 for Models 5a, 5b and 5c, respectively. The normalized RGB space measures the proportion of the color channels, rather than the signal intensity, which reduces negative effects caused by changes in illumination [11]. Models 5a-c produced r^2 values of greater than 0.92 for all five dyes, indicating that it is more color independent. Comparison between individual red, blue and green channel parameters shows that Model 5c (normalized blue channel), followed by Model 5a (normalized red channel), is the most linear model. This is because most digital image sensors, including cameras and smartphones, use the Bayer filter to detect color, where the green sensors as luminance-sensitive, while the red and blue sensors are chrominance-sensitive [30]. This makes the green channel more sensitive to lighting changes, while the red and blue channels are more sensitive to changes in color intensity. Therefore, the red and blue channels are more suitable for differentiating color due to concentration changes.

Model 6 utilized the HSL color space, which also attempts to minimize the effect of

lighting variation [11] by separating the lightness component (L) from the color values (Hue and Saturation). Model 6a (r^2 = 0.9815), which represents saturation or color intensity, is more robust than Model 6b (r^2 = 0.9423), which represents lightness. This is because a change in color intensity is a more reliable indicator of concentration change than a decrease in luminance. However, Models 5a and 5c still outperform Model 6a, possibly because the RGB to HSL conversion formula is unable to perfectly discriminate between the light and color components from the raw color data.

Overall, Model 5c, which is a normalized RGB model that uses all channel information for analysis, is the best performing linear color model for quantifying food dye concentration in solutions, with average values of 0.9935. This model can be applied to a wider range of food dyes with different color settings. It should be noted that the results demonstrate the significant impact of color model selection on the reliability and sensitivity of the DIA method. A multivariate approach and/or polynomial models can be considered especially for analyzing more complex samples. i.e dye mixtures, interacting samples.

Comparison between DIA and UV-Vis Spectroscopy Measurements

To verify the effectiveness of DIA measurements in analyzing a wider range of food dye colors, Model 5c was applied to all nine synthetic food dyes listed in Table 1. In addition, UV-Vis spectroscopy was conducted to compare the sensitivity of measurements (i.e. LOD and LOQ) obtained from DIA. The UV-Vis spectroscopy analysis involved plotting the absorbance maxima against the concentrations of the standard solutions, following the linear regression analysis employing Lambert-Beer-Bougert Law. The r^2, LOD and LOQ values were then determined from the linear regressions of both DIA and UV-Vis spectroscopy measurements, as presented in Table 3. The results indicate that both DIA (Model 5c) and UV-Vis spectroscopy can generate linear quantitative relationship to the dye concentration.

The r^2, LOD and LOQ values obtained from the DIA measurements as shown in Table 3 are generally consistent with those obtained from the UV-Vis spectroscopy measurements. The average r^2 values of the nine synthetic dyes obtained from DIA and UV-Vis spectroscopy measurements are 0.995 and 0.997, respectively. The corresponding limit of detection (LOD) and limit of quantification (LOQ) obtained from DIA for each food dye are following: carmoisine, 3.7 and 11.3 mg/L; sunset yellow, 1.0 and 3.1 mg/L; allura red, 2.0 and 6.0 mg/L; ponceau 4R, 1.3 and 4.0 mg/L; tartrazine, 5.0 and 15.2 mg/L; fast green, 2.0 and 6.1 mg/L; brilliant blue, 1.9 and 5.7 mg/L; quinoline yellow WS, 3.3 and 9.9 mg/L and indigo carmine, 1.2 and 3.8 mg/L. These LOD and LOQ values were comparable to those obtained from UV-Vis spectroscopy measurements (carmoisine, 2.4 and 7.2 mg/L; sunset yellow: 0.9 and 2.6 mg/L; allura red, 1.4 and 4.2 mg/L; ponceau 4R, 1.9 and 5.7 mg/L; tartrazine, 0.9 and 2.7 mg/L; fast green, 1.5 and 4.4 mg/L; brilliant blue, 3.6 and 10.9 mg/L; quinoline yellow WS, 0.3 and 0.9 mg/L and indigo carmine, 4.3 and 13.0 mg/L).

In general, the LOD and LOQ values obtained from the DIA measurements for the nine dyes range from 1.0 to 5.0 mg/L and 3.1 to 15.2 mg/L, respectively. The corresponding

LOD and LOQ values obtained from UV-Vis spectroscopy range from 0.3 to 4.3 mg/L and 0.9 to 13.0 mg/L, respectively. These results suggest that the DIA method, which offers ease of use and affordability, can achieve a similar level of sensitivity to the more established UV-Vis spectroscopy approach for analyzing food dyes, as evidenced by the comparable LOD and LOQ values. Therefore, the DIA method can serve as a viable alternative for quantitatively analyzing food dyes in solutions.

Table 3. The comparison of r^2, LOD (in mg/L) and LOQ (in mg/L) values between DIA (Model 5c) and UV-Vis spectroscopy measurements on various food dye solutions.

Dye	Concentration Range (mg/L)	Parameters	Linear Regression Analysis	
			DIA	UV-Vis
Carmoisine	0-50	r^2	0.9971	0.9988
		Slope	-0.0025	0.0419
		Intercept	0.3396	0.0106
		LOD	**3.7**	**2.4**
		LOQ	**11.3**	**7.2**
Sunset Yellow	0-30	r^2	0.9993	0.9995
		Slope	-0.0096	0.0461
		Intercept	0.3337	0.0093
		LOD	**1.0**	**0.9**
		LOQ	**3.1**	**2.6**
Allura Red	0-40	r^2	0.9986	0.9995
		Slope	-0.0045	0.0437
		Intercept	0.3336	0.0114
		LOD	**2.0**	**1.4**
		LOQ	**6.0**	**4.2**
Ponceau 4R	0-50	r^2	0.9996	0.9992
		Slope	-0.0034	0.0354
		Intercept	0.3382	0.0215
		LOD	**1.3**	**1.9**
		LOQ	**4.0**	**5.7**
Tartrazine	0-30	r^2	0.9837	0.9995
		Slope	-0.0059	0.0454
		Intercept	0.3247	-0.0097
		LOD	**5.0**	**0.9**
		LOQ	**15.2**	**2.7**
Fast Green	0-15	r^2	0.9907	0.9951
		Slope	0.0092	0.1278
		Intercept	0.3429	0.0482
		LOD	**2.0**	**1.5**
		LOQ	**6.1**	**4.4**
Brilliant Blue	0-20	r^2	0.9961	0.9859
		Slope	0.0103	0.1152
		Intercept	0.3396	0.0824
		LOD	**1.9**	**3.6**
		LOQ	**5.7**	**10.9**
Quinoline Yellow WS	0-25	r^2	0.9918	0.9999
		Slope	-0.0019	0.0597
		Intercept	0.3338	0.0031
		LOD	**3.3**	**0.3**
		LOQ	**9.9**	**0.9**
Indigo Carmine	0-50	r^2	0.9997	0.9962
		Slope	0.0058	0.0388
		Intercept	0.3336	0.0473
		LOD	**1.2**	**4.3**
		LOQ	**3.8**	**13.0**

Figure 3a depicts the characteristic linear quantitative relationship between normalized blue channel (Model 5c) and dye concentration, as determined by DIA measurement. Figure 3b shows the corresponding linear quantitative relationship between absorbance and dye concentration, as obtained through UV-Vis spectroscopy measurements. These illustrations are presented for carmoisine, tartrazine and brilliant blue dyes, which are analyzed in the commercial samples investigated in this study.

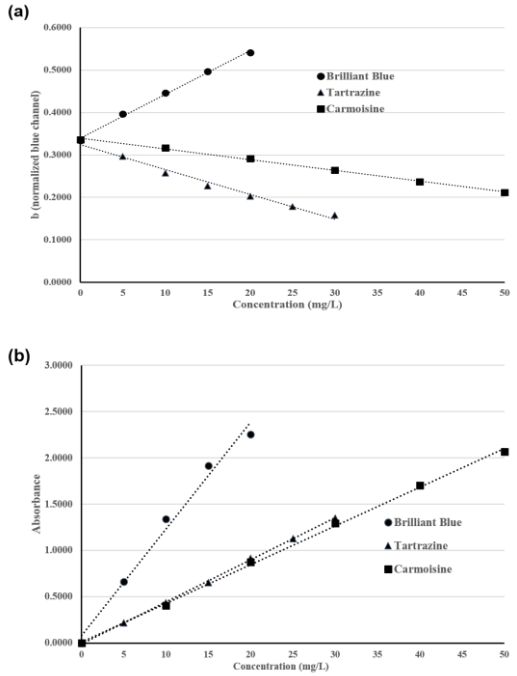

Figure 3. Calibration curves for carmoisine, tartrazine, and brilliant blue, obtained from (a) DIA using Model 5c (normalized blue channel) (b) UV-Vis spectroscopy.

Quantitative Determination of Food Dyes in Commercial Beverages

Some synthetic dyes pose serious health and safety risks, and this has led to federal oversight and restrictions, with the Food and Drug Act being passed in the US in 1906 [31]. Several studies indicate a number of positive carcinogenic, genotoxicity and hypersensitivity results demonstrated by several FDA-approved synthetic food dyes, including allura red, brilliant blue, sunset yellow and tartrazine [32]. In order to ensure public health and safety, it is imperative to analyze and monitor the use of appropriate synthetic food dyes and their allowable quantities used in commercial products.

To demonstrate the utility of DIA to assess food dye concentrations in commercial product, the quantitative analysis of three different commercial beverages (Samples S1, S2, and S3) was subsequently carried out using both DIA and UV-Vis spectroscopy methods. The three beverages contain carmoisine, tartrazine, and brilliant blue, respectively. The samples were directly analyzed using the sample preparation and measurement method as described in Method section. The UV-Vis spectroscopy measurements were used to validate the DIA measurement results. Before performing the quantitative analysis, a qualitative assessment was conducted by comparing the normalized spectra of each commercial sample solution to their corresponding standard solution spectra. Figures 4a-c show the comparison spectra of Samples S1-S3, respectively.

The comparison revealed that the maxima and shape of the sample and standard spectra are identical, affirming the identity of the dye used in each commercial sample and further indicating that there are no significant interactions between the dye and the other ingredients in all three commercial samples. This result implied that

the quantitative analysis is unbiased, and the obtained results can be attributed solely to the concentration of the dyes in the samples.

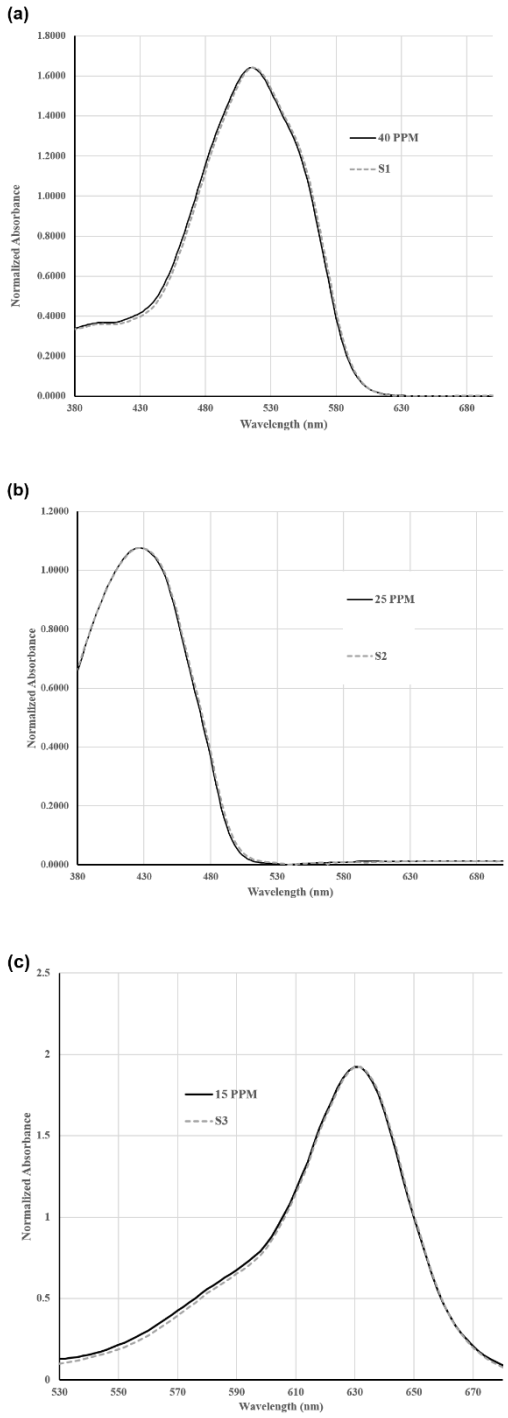

Figure 4. Comparison of normalized dye absorbance between standard solution and commercial samples (a) S1 (Carmoisine), (b) S2 (Tartrazine), and (c) S3 (Brilliant Blue).

The concentrations of food dyes in the commercial samples (S1, S2, and S3) were determined using both DIA based on external calibration and UV-Vis spectroscopy measurements based on external calibration and single-point standard addition method [26]. The single addition method was employed to validate the external calibration results.

All individual food dye concentrations used in the commercial samples were successfully determined using both DIA and UV-Vis spectroscopy measurements. Table 4 displays a satisfactory level of agreement between the dye concentration measurements in Samples S1-S3 obtained from both analytical techniques. The dye concentrations obtained from the three analytical methods, namely using DIA (external calibration using Model 5c) as well as UV-Vis Spectroscopy (external calibration) and single addition method, are highly consistent. The determined concentrations of carmoisine in Sample S1 are 52.7±2.6 mg/L, 53.7±0.1 mg/L, and 58.2±3.0 mg/L, respectively. Similar comparison results are achieved for Samples S2 and S3, as shown in Table 4. The measured concentrations of tartrazine in Sample S2 using DIA as well as UV-Vis Spectroscopy and single addition method are 105.9±4.3 mg/L, 100.7±1.5 mg/L, and 106.2±1.3 mg/L, respectively. The measured concentrations of brilliant blue in Sample S3 are 7.9±0.5 mg/L, 8.7±0.4 mg/L, and 8.3±0.5 mg/L, respectively. The accuracy of dye concentrations evaluated using the DIA differ by circa 0.3% (S2), 4.8% (S3) and to a maximum of 9.5% (S1), compared to those obtained from UV-Vis spectroscopy employing standard addition method.

Table 4. Comparison of food dye concentrations in commercial products (shown in bold), determined using DIA and UV-Vis spectroscopy methods.

Sample			Concentration (mg/L)		
Product	Dye	Lot	DIA (External)[1]	UV-Vis (External)[1]	UV-Vis (Std Addition)[2]
Strawberry-flavored soda (S1)	Carmoisine	1	10.5 ± 0.5 (52.3 ± 2.6)	10.5 ± 0.1 (52.4 ± 0.1)	11.9 ± 0.1 (59.6 ± 0.1)
		2	10.1 ± 0.4 (50.4 ± 1.8)	10.8 ± 0.1 (53.9 ± 0.1)	10.9 ± 0.1 (54.8 ± 0.1)
		3	11.1 ± 0.4 (55.6 ± 2.1)	11.0 ± 0.1 (54.9 ± 0.1)	12.0 ± 0.1 (60.2 ± 0.1)
		Mean	10.5 ± 0.3 **(52.7 ± 2.6)**	10.6 ± 0.1 **(53.7 ± 0.1)**	11.6 ± 0.6 **(58.2 ± 3.0)**
Energy drink (S2)	Tartrazine	1	22.0 ± 0.3 (110.2 ± 1.4)	20.1 ± 0.0 (100.5 ± 0.2)	10.7 ± 0.0 (107.0 ± 0.2)
		2	21.2 ± 0.2 (105.9 ± 1.2)	20.5 ± 0.0 (102.3 ± 0.1)	10.5 ± 0.0 (104.7 ± 0.4)
		3	20.3 ± 0.2 (101.6 ± 1.0)	19.9 ± 0.0 (99.3 ± 0.1)	10.7 ± 0.0 (106.9 ± 0.2)
		Mean	21.2 ± 0.9 **(105.9 ± 4.3)**	20.1 ± 0.3 **(100.7 ± 1.5)**	10.6 ± 0.1 **(106.2 ± 1.3)**
Blueberry-flavored soda (S3)	Brilliant Blue	1	8.4 ± 0.1	8.3 ± 0.1	7.8 ± 0.1
		2	8.0 ± 0.1	9.2 ± 0.1	8.7 ± 0.1
		3	7.3 ± 0.1	8.8 ± 0.1	8.5 ± 0.1
		Mean	**7.9 ± 0.5**	**8.7 ± 0.4**	**8.3 ± 0.5**

[1] Both samples S1 and S2 were diluted 5x for the DIA and UV-Vis measurements. The calculated concentrations of the original, undiluted sample were given in parentheses. Sample S3 was measured without dilution.
[2] Single-point standard addition analysis was performed by adding 0.1 mL of 1000 ppm standard solution to a 25 mL aliquot. Before adding the standard solution, Sample S1 was diluted 5x, while Sample S2 was diluted 10x to ensure that the concentrations of the measured solutions were within the linear concentration range. Sample S3 was measured without dilution.

One significant disadvantage of the current DIA color model compared to UV-Vis spectroscopy is that it cannot be used to distinguish different components in mixed dyes. However, when used to measure samples with simple matrices and a single-dye component, the results facilitate strong support for the reliability of the DIA using smartphone in evaluating synthetic dye concentrations present in commercial products and demonstrate the utility of DIA as an affordable tool for public health and safety monitoring.

CONCLUSION

This digital image analysis (DIA) study using smartphone assessed the performance of six color models on several food dyes representing different chemical structures and colors. The normalized blue channel (Model 5c) achieved the highest average r^2 value of 0.9935 and provided the lowest LOD and LOQ. This model is shown to be the most reliable DIA model that can be applied for various food dyes with different color settings. Further comparison with the more established UV-Vis approach demonstrated that the DIA method (using Model 5c) could achieve a comparable sensitivity level as shown by LOD and LOQ values on various food dyes from 1.0 to 5.0 mg/L and 3.1 to 15.2 mg/L, respectively, to those obtained from UV-Vis analysis (LOD: from 0.3 to 4.3 mg/L and LOQ: from 0.9 to 13.0 mg/L). Additionally, this study demonstrates the utility of DIA using smartphone for

quantitative analysis of food dyes in commercial products with simple matrices and containing single food dyes. The DIA method can reliably determine food dye concentrations in three commercial products and differ from 0.3% to less than 9.5% from those obtained from UV-Vis spectroscopy measurements. Overall, this color model study demonstrates the utility of DIA method as a reliable and affordable food dyes analysis tool that can potentially be used for public health and safety monitoring

ACKNOWLEDGEMENT

This work is supported under CIT Research Grant No. 2021-03-001.

REFERENCES

[1] R. Mustansar, "Smartphone-based optical and electrochemical sensing," *Smartphone-Based Detection Devices: Emerging Trends in Analytical Techniques*, pp. 19-36, 2021, doi:10.1016/B978-0-12-823696-3.00006-4.

[2] T. Lin, D. Lin, and L. Hou, "Fluorescence measurements, imaging and counting by a smartphone," *Smartphone-Based Detection Devices: Emerging Trends in Analytical Techniques*, pp. 57-72, 2021, doi:10.1016/B978-0-12-823696-3.00012-X.

[3] E. Bazani, M. S. Barreto, A. J. Demuner et al., "Smartphone Application for Total Phenols Content and Antioxidant Determination in Tomato, Strawberry, and Coffee Employing Digital Imaging," *Food Anal. Methods,* vol. 14, no. 4, pp. 631-640, 2020, doi: 10.1007/s12161-020-01907-z.

[4] F. Polat, "Development of a Simple and Accurate Analytical Method for the Determination of Nitrite in Processed Meat Products by Using an Optical Solid Chemosensor and Smartphone," *Food Anal. Methods*, vol. 15, no. 3, pp. 700-706, 2022, doi: 10.1007/s12161-021-02155-5.

[5] F. Böck, G. A. Helfer, A. B. da Costa et al., "Rapid Determination of Ethanol in Sugarcane Spirit Using Partial Least Squares Regression Embedded in Smartphone," *Food Anal. Methods,* vol. 11, no. 7, pp. 1951-1957, 2018, doi: 10.1007/s12161-018-1167-4.

[6] A. S. El-Sayed, H. Ibrahim, and M. A. Farag, "Detection of potential microbial contaminants and their toxins in fermented dairy products: A comprehensive review," *Food Anal. Methods*, vol. 15, no. 7, pp. 1880–1898, 2022, doi: 10.1007/s12161-022-02253-y.

[7] T. Sarkar, A. Mukherjee, K. Chatterjee et al., "Comparative Analysis of Statistical and Supervised Learning Models for Freshness Assessment of Oyster Mushrooms," *Food Anal. Methods*, vol. 15, no. 4, pp. 917-939, 2022, doi: 10.1007/s12161-021-02161-7.

[8] T. Sarkar, A. Mukherjee, K. Chatterjee, V. Ermolaev, D. Piotrovsky, K. Vlasova, M. Shariati, P. Munekata, and J. Lorenzo, "Edge Detection Aided Geometrical Shape Analysis of Indian Gooseberry (Phyllanthus emblica) for Freshness Classification," *Food Anal. Methods,* vol. 15, no. 4, pp. 917-927, 2022, doi: 10.1007/s12161-021-02206-x.

[9] Y. Fan "Digital image colorimetry on smartphone for Chemical Analysis: A Review," *Measurement*, vol. 171, p. 108829, 2021, doi:10.1016/j.measurement.2020.108829.

[10] H. Kim, J. H. Park, and H. Jung, "An Efficient Color Space for Deep-Learning Based Traffic Light Recognition," *J. Adv. Transp.*, 2018, doi: 10.1155/2018/2365414.

[11] E. Chavolla, D. Zaldivar, E. Cuevas, and Marco A. Perez, "Color Spaces

Advantages and Disadvantages in Image Color Clustering Segmentation," Advances in Soft Computing and Machine Learning in Image Processing, pp. 3-22, 2018, doi: 10.1007/978-3-319-63754-9_1.

[12] M. Firdaus, W. Alwi, F. Trinoveldi et al., "Determination of Chromium and Iron Using Digital Image-based Colorimetry," *Procedia Environ. Sci.*, vol. 20, pp. 298–304, 2014, doi: 10.1016/j.proenv.2014.03.037.

[13] S. Šafranko, P. Živković, A. Stanković et al., "Designing ColorX, Image Processing Software for Colorimetric Determination of Concentration, To Facilitate Students' Investigation of Analytical Chemistry Concepts Using Digital Imaging Technology," *J. Chem. Educ*., vol. 96, no. 9, pp. 1928-1937, 2019, doi: 10.1021/acs.jchemed.8b00920.

[14] J. Destino and K. Cunningham, "At-Home Colorimetric and Absorbance-Based Analyses: An Opportunity for Inquiry-Based, Laboratory-Style Learning," *J. Chem. Educ*., vol. 97, no. 9, pp. 2960-2966, 2020, doi: 10.1021/acs.jchemed.0c00604.

[15] T. Lerma, J. Martínez, and E. Combatt, "Determination of total protein content by digital image analysis: an approach for food quality remote analysis," *J. Sci. Technol. Appl.*, vol. 6, pp. 53-64, 2019, doi: 10.34294/j.jsta.19.6.41.

[16] A. Shalaby and A. Mohamed, "Sensitive Assessment of Hexavalent Chromium Using Various Uniform and Non-uniform Color Space Signals Derived from Digital Images," *Water Air Soil Pollut*., vol. 231, no. 10, 2020, doi: 10.1007/s11270-020-04891-6.

[17] M. Leulescu, A. Rotaru, A. Moanţă et al., "Azorubine: physical, thermal and bioactive properties of the widely employed food, pharmaceutical and cosmetic red azo dye material," *J. Therm. Anal. Calorim.,* vol. 143, no. 6, pp. 3945-3967, 2021, doi: 10.1007/s10973-021-10618-4.

[18] T. Güray, "Spectrophotometric determination of Sunset Yellow (E-110) in powdered beverages and pharmaceutical preparations after Cloud Point Extraction Method," *J. Turkish chem. soc. sect. chem.,* vol. 5, no. 2, pp. 479–492, 2018, doi: 10.18596/jotcsa.349382.

[19] K. Bevziuk, A. Chebotarev, D. Snigur et al., "Spectrophotometric and theoretical studies of the protonation of Allura Red AC and Ponceau 4R," *J. Mol. Struct*., vol. 1144, pp. 216-224, 2017, doi: 10.1016/j.molstruc.2017.05.001.

[20] F. Turak, M. Dinç, Öülger and M. Özgür, "Four Derivative Spectrophotometric Methods for the Simultaneous Determination of Carmoisine and Ponceau 4R in Drinks and Comparison with High Performance Liquid Chromatography," *Int. J. Anal. Chem*., pp. 1-11. 2014, doi: 10.1155/2014/650465.

[21] A. Asadzadeh Shahir, S. Javadian, B. B. Razavizadeh, and H. Gharibi, "Comprehensive study of tartrazine/cationic surfactant interaction," *J. Phys. Chem. B*, vol. 115, no. 49, pp. 14435–14444, 2011, doi: 10.1021/jp2051323.

[22] R.W. Sabnis, *Handbook of biological dyes and stains: Synthesis and industrial applications*. Hoboken, NJ: John Wiley & Sons, Inc., 2010, ISBN: 9780470586235.

[23] B. Tutunar, C. Tigae, C. Spînu, and I. Prunaru, "Spectrophotometry and electrochemistry of Brilliant Blue FCF in aqueous solution of NaX," *Int. J. Electrochem. Sci*., vol. 12, no. 5, pp. 3976-3987, May 2017, doi: 10.20964/2017.01.64.

[24] D. Snigur, M. Fizer, A. Chebotarev et al., "Protonation of quinoline yellow WS in aqueous solutions: spectroscopic and DFT theoretical studies," *J. Mol. Liq*., vol. 327, p. 114881, 2021, doi: 10.1016/j.molliq.2020.114881.

[25] M. Vidal and P. Freitas, "Kinetic Modeling of Adsorption of Indigo Carmine (5, 5'- Disulfonic Indigotin) on Peat," *Int. J. Adv. Res. Chem. Sci*., vol. 3, no. 3, pp. 25-36, 2016, doi: 10.20431/2349-0403.0303004.

[26] D. Harvey, "Calibrations, Standardizations, and Blank Corrections," in *Modern Analytical Chemistry.* Boston: McGraw-Hill, 2008, ISBN: 9780071169530.

[27] I. Porto, J. H. S. Neto, L. O. dos Santos et al., "Determination of ascorbic acid in natural fruit juices using digital image colorimetry," *Microchem. J*., vol. 149, p. 104031, 2019, doi: 10.1016/j.microc.2019.104031.

[28] T.F. Lin, "Experimental investigation of HSL color model in error diffusion," *2015 8th International Conference on Ubi-Media Computing (UMEDIA) Conference Proceedings*, pp. 268-272, 2015.

[29] A. V. Gerasimov, "Color Characteristics of Aqueous Solutions of Synthetic Food Dyes," *Russ. J. Appl. Chem.,* vol. 74, pp. 993–997, 2001, doi: 10.1023/A:1013029909630.

[30] B. Bayer, "Color imaging array," U.S. Patent No. 3,971,065, Jul. 20, 1975. No: US3971065A.

[31] I.D. Barkan, "Industry invites regulation: the passage of the Pure Food and Drug Act of 1906," *Am. J. Public Health*, 75(1), pp. 18-26, 1985, doi: 10.2105/ajph.75.1.18.

[32] S. Kobylewski and M. Jacobson, "Toxicology of food dyes," *Int J Occup Environ Health,* vol. 18, no. 3, pp. 220-246, 2012, doi:10.1179/1077352512Z.00000000034.